

AperTO - Archivio Istituzionale Open Access dell'Università di Torino

Biodegradable microparticles designed to efficiently reach and act on cystic fibrosis mucus barrier

This is a pre print version of the following article:

Original Citation:

Availability:

This version is available <http://hdl.handle.net/2318/1698755> since 2019-04-17T12:33:15Z

Published version:

DOI:10.1016/j.msec.2018.10.064

Terms of use:

Open Access

Anyone can freely access the full text of works made available as "Open Access". Works made available under a Creative Commons license can be used according to the terms and conditions of said license. Use of all other works requires consent of the right holder (author or publisher) if not exempted from copyright protection by the applicable law.

(Article begins on next page)

Biodegradable microparticles designed to efficiently reach and act on cystic fibrosis mucus barrier

Caterina Cristallini^a, Nicoletta Barbani^b, Letizia Ventrelli^{b,c}, Chiara Summa^b, Sara Filippi^b, Tania Capelôa^c, Emanuela Vitale^c, Carlo Albera^{c,d}, Barbara Messori^d, Claudia Giachino^c

^aNational Research Council CNR, Institute for Chemical and Physical Processes, IPCF uos Pisa, c/o Largo Lucio Lazzarino 2, 56124 Pisa, Italy

^bUniversity of Pisa, Department of Civil and Industrial Engineering, Largo Lucio Lazzarino 2, 56124 Pisa, Italy

^cUniversity of Turin, Department of Clinical and Biological Sciences, Regione Gonzole 10, 10043 Orbassano (Turin), Italy

^dOspedale San Luigi, Adult Cystic Fibrosis Centre, Regione Gonzole 10, 10043 Orbassano (Turin), Italy

*Corresponding author at: CNR, Institute for Chemical and Physical Processes, IPCF uos Pisa, c/o Largo Lucio Lazzarino 2, 56124 Pisa, Italy.

E-mail address: caterina.cristallini@cnr.it (C. Cristallini).

Abstract

Cystic fibrosis (CF) is a progressive genetic disease caused by mutations in the gene that produces the CF transmembrane conductance regulator (CFTR) protein. The malfunction of the CFTR protein causes a thick buildup of mucus in the lungs that clogs the airways and traps bacteria, thus leading to infections, extensive lung damage and respiratory failure. Micro-delivery systems are currently being investigated as an efficient way to cross the viscous and complex architecture of the CF mucus. In this study, we produced synthetic and natural microparticles (MPs) based on poly(DL-lactide-co-glycolide) (PLGA) or gellan gum through tailored water/oil emulsion procedures. Morphological and physico-chemical characterizations were carried out on both classes of MPs showing particles having diameters within suitable ranges to reach the CF airways. *In vitro* biocompatibility tests were also performed on both MPs using a human lung cancer cell line (A549) demonstrating that treatment with MPs induces no cytotoxic effects. Both classes of MPs were loaded with a mucolytic agent (N-acetyl

cysteine, NAC) and their release kinetics evaluated using high performance liquid chromatography (HPLC). The analysis pointed out that the amount of NAC released from MPs resulted in a dose-dependent increment, with a rapid release kinetic to satisfy the requirement for inducing an early mucus degradation. Finally, mucolytic action of NAC-loaded MPs was evaluated in an artificial sputum model through its rheological analysis obtaining the lowest viscosity profile after the addition of drug-loaded MPs. Taken together, gained results allowed us to select suitable MPs as potential drug targeting platforms having a mucolytic action for CF treatment.

Keywords

Drug delivery systems; microparticles; cystic fibrosis; biocompatible polymeric materials; N-acetyl cysteine; artificial sputum.

1. Introduction

Cystic fibrosis (CF) is an autosomal recessive systemic disease, which is the result of a genetic defect in the CF transmembrane conductance regulator (CFTR) gene. Pulmonary disease accounts for over 90% of the morbidity and mortality associated with the disease. Since one of the physiological functions of CFTR is to inhibit the epithelial sodium channel, a lack of CFTR activity leads to decreased chloride secretion as well as sodium hyperabsorption [1]. The result of the malfunction of these transmembrane channels in CF is a decreased airway surface liquid (ASL) volume, which leads respiratory cilia to collapse and the impaired mucus detachment from the submucosal gland ducts in the conducting airways [2], as well as the impaired mucociliary clearance and mucus retention in the lower airways. Indeed, mucus in the lungs of CF patients becomes thick and sticky clogging their airways and trapping bacteria [3, 4], which result in the vicious cycle of recurrent/persistent bacterial infections, chronic inflammation and pulmonary exacerbations [5, 6]. Therefore, these conditions predispose patients with CF to the progressive loss of pulmonary function, respiratory failure and consequently death [7].

At present there is no cure for CF, but advances in pharmacotherapy have gradually increased the life expectancy of CF patients. The main stay of the current approach to treat CF has been symptomatic therapy aimed at attenuating disease progression and delaying the onset of irreversible lung damage [8- 11]. Anti-inflammatory drugs and antibiotics are administered to control the airway inflammation and infection due to several bacterial pathogens (such as *Pseudomonas aeruginosa* [12- 14]). Numerous data suggest that the use of standard drug dosages result in sub-optimal drug concentrations at the site of infection [15] due to both low concentrations of antibiotics at the site of infection [16] and the increased tolerance of bacterial biofilms to antibiotics [17- 19]. Bronchodilators

are used to control bronchial hyperactivity and to improve sputum clearance and airflow through the diseased airway, whilst mucolytics and osmotic agents followed by chest physical therapy have been effective in improving airway clearance. Following identification of the CFTR gene, gene therapy has been explored as a fundamental CF therapy at investigational levels and a realistic therapeutic opportunity rely on the possibility to enhance CFTR activity with CFTR modulators and correctors. [20, 21].

As the airways are the major therapeutic target in CF, many CF drugs are delivered via inhalation thus providing an attractive mode of delivery of existing and emerging therapeutic agents. Given that an inhaled-based antibiotic therapy delivers the drug directly to the desired site of action hence diminishing side effects, it represents a desirable alternative to oral or parenteral therapy. However, several challenges need to be overcome for an efficient inhalational drug delivery to the CF lungs. Among these, improvements in terms of geometric particle sizes, powder flowability and respirable fractions are required. Nevertheless, particular attention at level of the underlying epitheliums has to be also paid to the dehydrated, thick and tenacious CF sputum in order to ensure an effective inhalational delivery of many therapeutic agents [22, 23]. The failure of CF gene therapy in the past 15 years of preclinical and clinical research is clear proof of the delicate role played by CF sputum [24].

New approaches have been proposed aimed at increasing the mobility of administered drug formulations through the tenacious CF sputum or increasing drug access to the therapeutic target. To achieve high local medicine concentrations, especially in the paranasal sinuses and in sputum, new delivery forms of the already available antibiotics and anti-inflammatory agents are indeed needed. Recently, novel drug delivery systems (NDDSs) based on nano entities, micro entities or a combination of them have been explored because they offer concrete benefits in terms of reduced dosing frequency, increased bioavailability, prevention from degradation, site specificity and reduced side effects [25, 26]. *In vitro*, *ex vivo* and *in vivo* findings of numerous worldwide experimentations strongly suggested NDDSs as an emerging and promising option to combat major disorders/diseases [27, 28]. Concerning nanomedicine, the use of its principles and strategies is gaining researchers' attention with highly promising perspectives in several fields such as diagnosis and treatment of pediatric disorders and genetic deficiencies (e.g. CF) [29]. The strategy of using nanocarriers encapsulating locally-acting drugs at pulmonary level indeed provides several advantages for the treatment of respiratory diseases and CF [30- 36]. The benefits include sustained drug delivery to the lungs, reduced therapeutic dose and improved patient compliance. However, some challenges have to be taken into account such as the understanding of the factors governing the mucus penetration

capability of nanocarriers or the identification of new technologies for delivering drugs to specific regions/cell types of the lungs.

Parallel to nanomedicine, scientists are also exploring additional strategies based on micro entities, which represent the main focus of the present study. Therapies based on microparticles (MPs) systems allow tailored drug release to the specific treatment site and formulation of various drug–polymer combinations. Moreover, microparticulate-based vehicles help in maintaining the therapeutic concentration of drugs (i.e. shorter half-life) in plasma for longer period of time by controlling their release. MPs have also large surface-to-volume ratios thanks to their small size and can be developed for the improvement of dissolution rate of practically insoluble drugs. To attain optimal therapeutic concentrations of drug in circulatory system, specific parameters such as dose and release kinetic can be manipulated time to time as per the requirement by employing specific microencapsulation methods, varying drug–polymer ratio, etc. [37]. As reported in literature, several drug-loaded microparticulate systems have been developed for their oral [38], topical [39], parenteral [40] and nasal [41] administration.

With the aim to investigate MPs as vehicles to penetrate the viscous and highly complex CF mucus barrier hence targeting precise regions of the lungs, particular attention has therefore to be paid to the specific therapeutic agents that can be loaded onto such micro systems. To improve sputum clearance and then lung function, mucolytic agents (such as acetyl cysteine, dornase alfa, mannitol, etc.) are currently used since they influence mucus rheology by cleaving its components thus reducing the viscosity of CF sputum and enhancing drug penetration [42, 43]. Yang *et al.* [44] for example produced mannitol MPs as carriers of ciprofloxacin and showed its enhanced diffusion as well as its anti-pseudomonal effect in a sputum-like material. Another commonly used mucolytic agent is N-acetyl cysteine (NAC) that acts by cleaving disulphide bonds of mucin fibers, thus reducing the viscosity of mucus/sputum *in vitro* and *in vivo* [45]. Among several interesting papers focusing on NAC action, Suk *et al.* [46] tested the use of such mucolytic agent as an adjuvant to enhance particle transport through CF sputum. Specifically, the authors demonstrated that only the simultaneous treatment with both NAC and particles possessing muco-inert coatings could enhance their penetration across sputum of CF patients.

Recognizing all the aspects previously described, in this study we explored hydrophilic and bioresorbable materials based on natural and biodegradable synthetic polymers to produce MPs, in association with the de-polymerizing drug NAC, to evaluate their potential in reducing mucin-glycocalix adhesion [47] and therefore increasing the spacing of the dense CF sputum mesh. The production of MPs was optimized to have suitable dimensions in agreement with the airway size and

anatomy, thus for their correct local deposition and distribution. Physico-chemical characterizations of both non-loaded MPs (hereinafter referred to as unloaded MPs) and NAC-loaded MPs were carried out using differential scanning calorimetry (DSC), thermogravimetric analysis (TGA) and Fourier transform infrared (FT-IR) spectroscopy to assess the effective absorption and distribution of the mucolytic drug on MPs surface. Before evaluating the effect of loaded MPs on mucus degradation, artificial sputum (AS) was produced and its rheological properties compared with sputum from CF patients. Rheological analysis was carried out to assess the influence of NAC on the AS viscosity after the addition of NAC-loaded MPs. Viscosity measurements were also performed on both AS loaded with MPs without NAC and AS loaded directly with the drug. Finally, *in vitro* release tests of NAC from the two different MP systems were performed using HPLC to evaluate their release kinetics.

2. Materials and methods

a. Materials

Poly(DL-lactide-*co*-glycolide) acid (PLGA; lactide glycolide 50:50 with $M_w = 40,000-75,000$), poly(vinyl alcohol) (PVA; average $M_w = 13,000-23,000$ with 87-89% hydrolysis), NAC ($\geq 99\%$, $M_w = 163.19$ g/mol), egg yolk L- α -Phosphatidylcholine (PC), dichloromethane (DCM $\geq 99.9\%$), and 2-Propanol (ISO $\geq 99.8\%$) were purchased from Sigma-Aldrich (St. Louis, USA). Gellan gum (GL) was bought from Fluka Chemicals (Buchs, Switzerland), whereas acetonitrile (ACN $\geq 99.9\%$) was purchased from Honeywell Research Chemicals (Morris Plains, USA).

2.2 Preparation of MPs

Two different classes of MPs based on a hydrophilic biodegradable synthetic copolymer (PLGA) and a natural water-soluble polysaccharide (GL) were prepared according to slightly different procedures compared to those previously reported in literature by the authors' research team [48, 49]. In particular, the production of PLGA and GL biodegradable MPs was carried out through two different procedures based on the oil-in-water (O/W) single-emulsion technique and the water-in-oil (W/O) emulsion method, respectively, using specific surfactant agents. The experimental conditions, in terms of polymer concentrations, solvents (DCM, water), stirring rate, time and temperature, were optimized to obtain MPs with suitable dimensions in agreement with the CF airway calibre and anatomy, thus being able to reach the mucus layer.

To produce both PLGA and GL MPs, a reaction system based on a three-necked round-bottom glass flask was used to contain the solutions. The mechanical stirring of the prepared mixtures was performed by means of a Heidolph RZR 2020 stirrer (50 W powered motor with speed range 40-

2,000 rpm by Heidolph Instruments GmbH & Co. KG, Germany) equipped with a glass shaft ensuring their constant and homogeneous agitation. A bulb condenser connected to one neck of the flask was also used during GL MPs fabrication to avoid the evaporation of the solvent.

PLGA microspheres

Firstly, a 2.5% (w/v) PVA solution was prepared in a reaction system by dissolving 5 g of PVA in 200 mL of MilliQ water; subsequently, a solution containing 600 mg of PLGA in 10 mL of DCM (6% w/v) was added to the PVA solution previously prepared. The O/W solution was mechanically stirred at 800 rpm for 2 h in order to obtain a micro-emulsion. The stirring of the solution was therefore continued overnight at 200 rpm and the flask opened to allow solvent to evaporate. The excess of PVA was removed by several washing steps ($5 \times 40 \text{ mL} \times 5 \text{ min}$) in MilliQ water followed by centrifuging (4235-ALC centrifuge, Winchester, USA) at 5,000 rpm for 5 min. The MPs suspension was then freeze-dried via a lyophilisation process, and the PLGA microspheres obtained were finally stored in a desiccator at room temperature until their use.

GL microspheres

A solution of DCM containing 1.5% (w/v) of PC as an emulsifier was prepared by dissolving 3 g of PC in 200 mL of DCM, and subsequently poured into the reaction system immersed in an oil bath. Simultaneously, 300 mg of GL powder was dissolved in 40 mL of deionized water (0.75% w/v) at 50°C. Once the temperature of the oil bath reached 50°C, the hot GL solution was slowly added inside the flask under stirring at 500 rpm. The resulting emulsion was then stirred at 800 rpm for 30 min at 50°C and 2 h at room temperature. Afterwards, the stirring rate was reduced to 300 rpm and the flask was moved in an ice bath for 30 min. The mixture was finally incubated at 4°C overnight so that the gelling mechanism could occur. Particles recovery was obtained by washing steps ($10 \times 50 \text{ mL} \times 15 \text{ min}$) with ISO in order to remove the remaining PC. Finally, GL MPs were dried under the hood and stored at room temperature until their use.

Drug loading

To prepare drug loaded MPs, the mucolytic drug NAC was used, as it is a depolymerizing agent commonly used for the reduction of the viscosity of CF sputum. In this study, aqueous solutions of NAC were initially prepared using three different concentrations, namely 0.3, 1, 3 mg/mL (w/v), by dissolving the drug in MilliQ water. Therefore, small quantities of both PLGA and GL microspheres were added to each of the NAC solutions and left for 2 h at room temperature in order to allow drug absorption. MPs dispersions were then centrifuged at 14,000 rpm for 10 min using a Microcentrifuge 4214, and the supernatants were removed and stored at 4°C. Supernatants were

subsequently analyzed by HPLC (for details, see Section 2.4) to evaluate the total amount of absorbed NAC as a function of the tested concentrations, and hence to select the proper one to be used for the following characterizations. Finally, the remaining NAC-loaded PLGA and GL microspheres were recovered after drying in ventilated oven at 30°C to completely remove the excess of water, and later used to test *in vitro* biocompatibility as well as their mucolytic activity. Unloaded MPs were also prepared as control.

2.3 *In vitro* drug release

PLGA MPs and GL MPs loaded with the three different concentrations of NAC (that is 0.3, 1 and 3 mg/mL (w/v)) were dispersed in MilliQ water and at prefixed times (5, 10, 20, 30, 60, 120 min, 5 and 24 h) each sample was centrifuged at 14,000 rpm for 10 min. Supernatants were then removed and replaced with fresh MilliQ water. All the collected samples were later analyzed by HPLC (for details, see Section 2.4) to assess release kinetics.

2.4 Characterizations of MPs

After MPs fabrication and drying, the yield was determined by weighing the microspheres recovered and calculating the percentage yield with respect to the initial amount of polymers which had been used for their production as follows:

$$\text{Percentage yield} = W_{\text{MPs}}/W_{\text{P}} \times 100$$

where:

W_{MPs} = total amount of produced MPs;

W_{P} = initial amount of polymer.

Subsequently, morphological analysis of PLGA and GL MPs was carried out using a JEOL JSM 5600 scanning electron microscope (SEM; Tokyo, Japan) onto gold-sputtered particles. The size of a minimum of 100 randomly selected particles was calculated from the acquired SEM digital images using the image analysis ImageJ software (free download from NIH, <http://rsbweb.nih.gov/ij/>). Both unloaded and NAC-loaded PLGA and GL microspheres were then characterized through DSC (DSC-7 instrument, Perkin Elmer, USA) by introducing small quantities of particles into aluminium pans and scanning them with a heating rate of 10°C/min at different temperature ranges (i.e. 20-200°C for PLGA MPs and 20-270°C for GL MPs) in nitrogen flow. Moreover, TGA was performed on both unloaded and drug-loaded MPs using a TGA 6 analyser from Perkin Elmer. Small amounts of particles were placed into ceramic capsules and analysed from 30°C to 500°C at a heating rate of 10°C/min in nitrogen flow; the effective NAC loading was therefore estimated by the weight losses

of the samples as a function of temperature. As a reference, TGA was also performed on pure NAC. Chemical analysis on pure NAC, unloaded and NAC-loaded PLGA and GL MPs were carried out by FT-IR Chemical Imaging (Perkin Elmer Spotlight 300, USA) in order to obtain chemical and correlation maps allowing to evaluate the distribution of the pure components inside the material. Spectral images were acquired both in transmission and attenuated total reflectance (μ ATR) mode (spectral resolution of 4 cm^{-1} , spatial resolution of $100 \times 100\ \mu\text{m}$) using the infrared imaging system Spotlight 300 from Perkin Elmer. In particular, spectra generated from the surface layer of the samples were collected by pressing MPs powder into direct contact with the ATR crystal. The amounts of both absorbed and *in vitro* released NAC from PLGA and GL MPs were determined through a chromatographic analysis of the previously collected solutions by HPLC at a wavelength $\lambda = 215\text{ nm}$ (Synergy Hydro C18 column, Perkin Elmer series 200 UV/VIS detector, PerkinElmer series 200 pump). A mixture of MilliQ: ACN (93:7, v/v) was used as mobile phase at a flow rate of 1 mL/min and the volume of liquid injected was $100\ \mu\text{L}$.

2.5 Biocompatibility *in vitro* tests

The human lung cancer cell line A549 (American Type Culture Collection, Manassas, USA) was cultured in complete Dulbecco's Modified Eagle's Medium (DMEM; $1,000\text{ mg/L}$ glucose) (Sigma-Aldrich) supplemented with 10% fetal bovine serum (FBS) (Sigma-Aldrich), 2 mM L-Glutamine, 1% kanamycin, 1% sodium pyruvate, 1% nonessential amino acids, 0.1% β -mercaptoethanol (all components from Gibco, Gaithersburg, USA). Cells were maintained in a humidified atmosphere with 5% CO_2 at 37°C and then subcultured twice a week. For cell viability and proliferation assays $20,000\text{ cells/cm}^2$ were seeded in 6-multiwell plates and allowed to attach overnight. Thereafter, cells were treated with 10 and $100\ \mu\text{g/mL}$ concentrations of PLGA and GL MPs diluted in bidistilled water. Cells treated with the same amount of bidistilled water were used as control.

Cell viability was evaluated by propidium iodide (PI) (Sigma-Aldrich) staining at 24, 48 and 72 h after cell treatment. Specifically, cells were collected, resuspended in phosphate-buffered saline (PBS) at 10^6 cells/mL and stained with $1\ \mu\text{g/mL}$ PI for 5 min at room temperature in the dark. At least 20,000 events for each experimental time point were acquired on a Cyan ADP flow cytometer (Beckman Coulter, Brea, USA) and analysed with Summit 4.0 software. Viable cells were expressed as percentage of living cells, evaluated on PE-log vs FS-Lin plots, and normalized respect to the relative time-point control.

Cell proliferation was evaluated at the same time points (i.e. 24, 48 and 72 h) by cell counting. In particular, cell number was estimated by treating the cells with trypsin-EDTA solution 0.25% (Sigma-

Aldrich) and subsequently placed in a counting chamber Neubauer-improved (Marienfeld-SupeRior, Germany) in order to be counted using an optical microscope (Motic AE2000TRI, Barcelona, Spain).

2.6 Patients mucus collection

Sputum samples were collected from 2 adult CF patients (age 27 and 35 yr) with chronic *P.aeruginosa* respiratory chronic infection, attending outpatient clinics at San Luigi Hospital and who were receiving DNase therapy. Samples were spontaneously expectorated and stored at -80°C prior to use in experiments.

2.7 Preparation of AS

Preparation of AS was carried out according to Ibrahim *et al.* [49]. Briefly, for 50 mL of AS, 500 mg of deoxyribonucleic acid (DNA; Sigma-Aldrich) from salmon testes was dissolved in 32.5 mL DNase-free water (Life Technologies), supplemented with 250 μL of egg yolk emulsion (Sigma-Aldrich). Apart, 250 mg mucin type II from porcine stomach (Sigma-Aldrich) was dissolved in 5 mL of MilliQ water, and 0.295 mg of diethylenetriaminepentaacetic acid (DTPA; Sigma-Aldrich), 250 mg NaCl, 110 mg KCl, and 22 amino acids (12.5 mg each) (Fluka) in 12.5 mL of MilliQ water. After mixing all the three solutions, the pH was set to 7 with 1 M NaOH. To prolong the AS storage-life, the solutions were filtered and 0.4 $\mu\text{L}/\text{mL}$ penicillin-streptomycin and 1 $\mu\text{L}/\text{mL}$ ampicillin (Sigma-Aldrich) were added.

2.8 Rheological analysis of CF patients mucus and AS

Preliminary rheological tests were firstly carried out on CF patient sputum, pure AS and AS loaded with two different concentrations of PLGA and GL MPs, namely 5 mg/mL and 100 $\mu\text{g}/\text{mL}$, in order to find the proper experimental conditions for the later analysis.

Therefore, the effects of the mucolytic agent on AS degradation were evaluated on a series of samples using 2 mL of AS, an aqueous solution of NAC at 3 mg/mL (w/v) and 10 mg of MPs, as follows: pure AS, AS loaded with PLGA or GL MPs without NAC, AS loaded directly with NAC solution and AS loaded with PLGA or GL MPs containing NAC. MPs were firstly hydrated with a small amount of water before adding the mucus and incubated for 2 h at 37°C . Specimens were therefore prepared by pouring 2 mL of fluid sample into individual conic moulds (40 mm diameter). Rheological measurements were performed on 30 samples by means of a rotational rheometer Kinexus (Malvern, UK). The Shear Rate Ramp Linear sequence, that calculates viscosity vs shear rate, was used by setting the temperature at 37°C , a start shear rate of 0.1 s^{-1} and an end shear rate of $1,000\text{ s}^{-1}$.

2.9 Statistical Analysis

The experimental results reported in this study are expressed as mean \pm standard deviation (SD). Student's *t* test was used to evaluate the effect of MPs on cell viability and proliferation, and statistics were calculated using GraphPad Prism 5.0 (GraphPad Software, San Diego, USA). The level of significance was $p < 0.05$ and *n* corresponds to the number of independent experiments.

3 Results and Discussion

3.1 Characterizations of MPs

3.1.1 Percentage yields

After the drying step and before their use, the percentage yields of PLGA MPs and GL MPs were calculated obtaining 89% w/w and 96% w/w, respectively, thus showing a small loss of both the polymers during MPs production and the particles themselves during their recovery.

3.1.2 Morphological analysis

The morphology of particles obtained through the W/O emulsion technique was at once analysed using SEM (Figure 1). Both PLGA and GL MPs present a spherical shape that optimizes the surface-to-volume ratio, thus providing appropriate carriers for drug delivery.

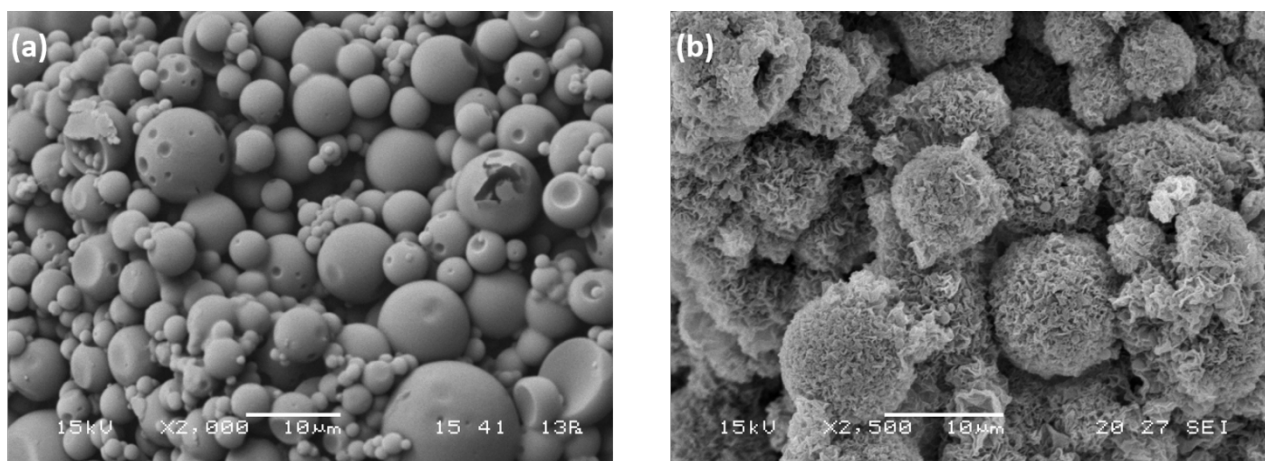


Fig.1 SEM images of PLGA MPs under 2,000 \times magnification (a) and GL MPs under 2,500 \times magnification (b).

Figure 1a shows the SEM image of PLGA MPs having a smooth surface and diameters of $5.48 \pm 1.5 \mu\text{m}$. Figure 1b illustrates the SEM image of GL MPs with diameters of $7.37 \pm 1.83 \mu\text{m}$ but a porous surface. It is well known [51] that particle size along with shape and surface structure are important parameters strictly connected to the therapeutic effect of the drug-loaded carriers when inhaled via dry powder inhalers (DPIs). In particular, particles with a diameter below $1\text{-}3 \mu\text{m}$ are mostly exhaled upon inhalation, whereas those with a diameter higher than $10 \mu\text{m}$ are mainly deposited in the large

conducting airways and oropharyngeal region without reaching the specific lung tissue for a correct drug release [7]. Therefore, MPs obtained directly by the production phase showed a diameter in a range compatible with the specific application, however it is possible to further select MPs groups with a selected average diameter by using specific sieves in order to satisfy requirements for an appropriate DPI design. Concerning surface structure of particles, the sponge-like morphology of GL MPs is important since it is responsible for their high capability to swell in water and rapidly dissolve into mucus. Moreover, porosity can be used to enhance both the absorption of the drug and its deposition. As regards drug absorption, porous particles with the spheroidal shape allow a higher amount of drug to be adsorbed throughout the surface [52]. In relation to drug deposition and release, it has been demonstrated that large porous particles (LPPs) possess optimized flow properties [53, 54]. In fact although they exhibit large geometric size, LPPs show small aerodynamic size which results from their low density, allowing them to overcome upper airways, escape phagocytosis by alveolar macrophages and penetrate deep into the lungs for an efficient therapeutic treatment.

3.1.3 Physico-chemical analysis

A complete physico-chemical characterization of PLGA MPs and GL MPs was carried out before and after NAC loading by using HPLC, DSC, TGA and FT-IR Chemical imaging.

NAC-loaded PLGA MPs

The loading of PLGA MPs with NAC at three different concentrations, namely 0.3, 1 and 3 mg/mL (w/v), was found to increase in a dose-dependent manner reaching the maximum loading efficiency (>80%) at 3 mg/mL. Therefore, the obtained result allowed us to select this last as the definitive drug concentration.

To confirm the effective loading of the mucolytic agent into PLGA MPs, a direct analysis of both unloaded particles and particles loaded with 3 mg/mL of NAC was performed through DSC and TGA analysis.

Figure 2a shows DSC-thermograms of PLGA MPs before and after NAC loading. The glass transition temperature (T_g) was observed at about 57°C for pure PLGA MPs, whereas in the case of particles carrying NAC it was at about 54°C. The shift of the T_g of the synthetic polymer PLGA to slightly lower temperature for NAC-loaded samples with respect to unloaded MPs suggested a plasticizing effect due to the mucolytic agent.

TGA (and the corresponding derivative curves) for unloaded PLGA MPs and NAC-loaded PLGA MPs are reported in Figure 2b. A shift of the maximum degradation rate towards higher temperatures

for NAC-loaded particles (i.e. $\sim 359^\circ\text{C}$) compared to the unloaded ones (i.e. $\sim 353^\circ\text{C}$) was recorded, which could be ascribed to the presence of the drug inside MPs.

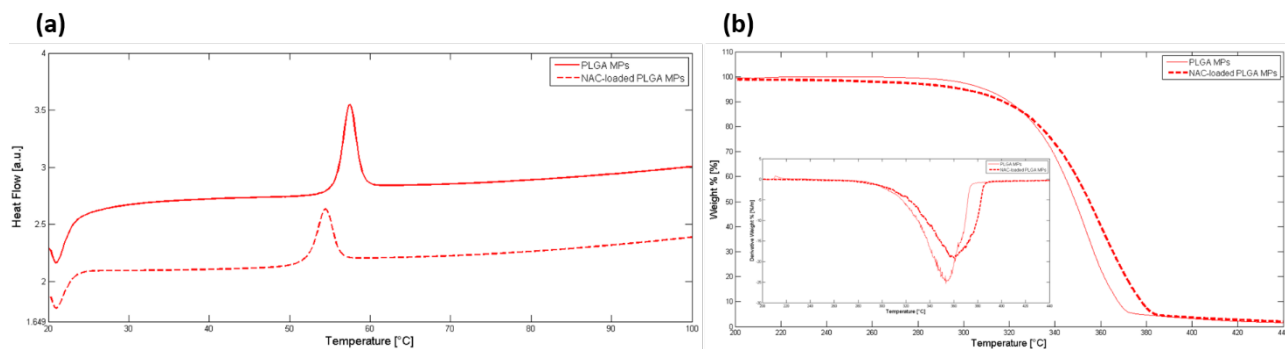


Fig.2 Characterizations of PLGA MPs unloaded and loaded with NAC: DSC-thermograms (a) and TGA curves (b). a.u.: arbitrary units; inset: second derivative traces obtained from TGA.

Finally, FT-IR analysis was carried out on PLGA MPs containing the mucolytic agent in order to assess the real drug loading inside the particles. Firstly, IR spectra of pure NAC and PLGA MPs were acquired to identify their characteristic absorption bands. In particular, FT-IR spectrum of NAC showed the following peaks: O-H stretching at $3.110\text{-}1.800\text{ cm}^{-1}$, N-H stretching at 3.400 cm^{-1} , C=O stretching at $1.700\text{-}1.750\text{ cm}^{-1}$, N-H bending at 1.600 cm^{-1} . Concerning PLGA, FT-IR spectrum revealed the following peaks: CH, CH₃ and CH₂ stretching at $3.000\text{-}2.700\text{ cm}^{-1}$, C=O stretching at $1.900\text{-}1.550\text{ cm}^{-1}$, CH₃ and CH₂ deformation at $1.500\text{-}1.250\text{ cm}^{-1}$, CH₂ and CH vibration at $1.350\text{-}1.150\text{ cm}^{-1}$, C-O stretching at $1.300\text{-}1.150\text{ cm}^{-1}$. Afterwards, FT-IR analysis both in μATR and transmission mode was performed on PLGA MPs before and after NAC loading. Analysis carried out in μATR mode did not show the presence of the drug on the particles surface (data not shown). On the contrary, analysis made in transmission mode revealed NAC inside PLGA MPs. Figure 3 illustrates transmission maps of NAC-loaded PLGA MPs (Fig. 3a and b) and the corresponding medium spectrum (Fig. 3c). The characteristic peak of PLGA at 1.750 cm^{-1} was due to the C=O stretching of the ester group, whilst those characteristic of NAC were found at 1.726 and 1.620 cm^{-1} . Furthermore, the presence of NAC was clearly proved by the yellow zone below the surface of the drug loaded microspheres.

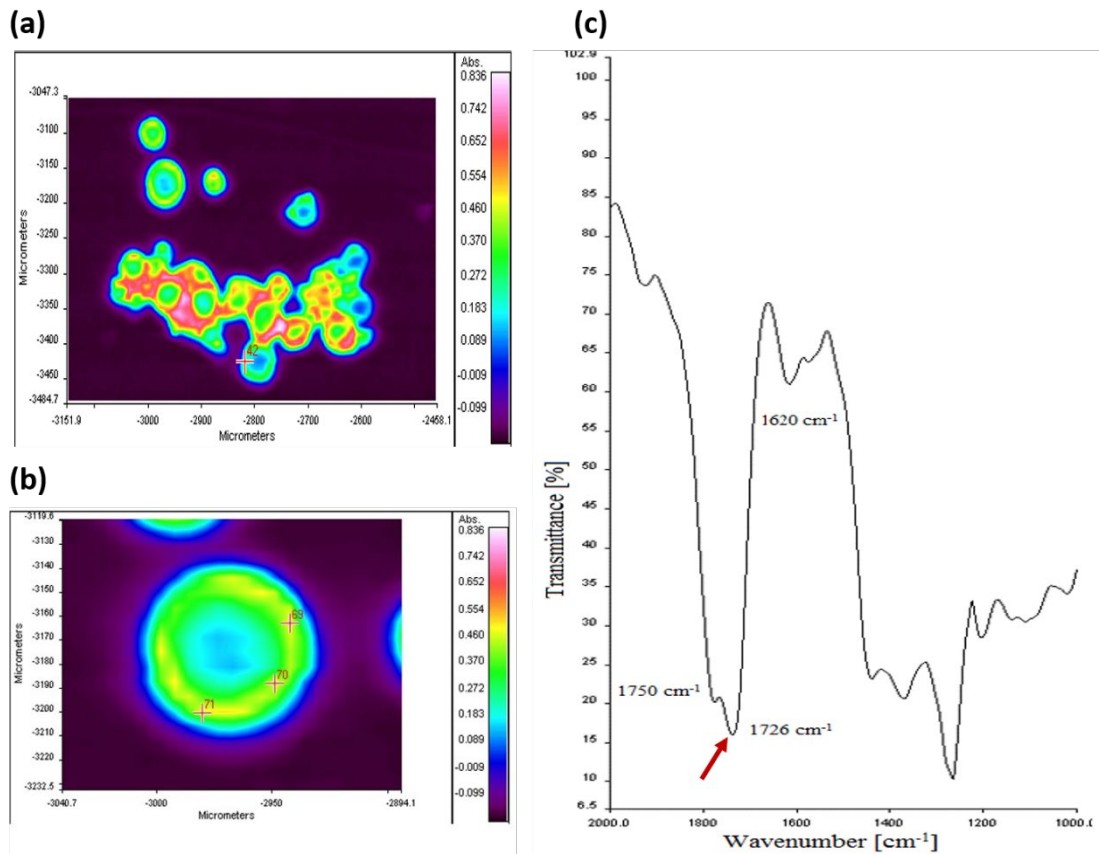


Fig.3 Chemical map (a), a detail (b) and medium spectrum (c) obtained in transmission mode of NAC-loaded PLGA MPs.

NAC-loaded GL MPs

After the loading phase of NAC into GL MPs using three different concentrations (i.e. 0.3, 1 and 3 mg/mL (w/v)), the amount of drug absorbed into particles was found to increase in a dose-dependent manner with the maximum corresponding to 3 mg/mL and a loading efficiency >70%. As for PLGA MPs, the gained result permitted to choose such concentration as the final drug concentration.

Results obtained from DSC and TGA analysis carried out on both unloaded and NAC-loaded (3 mg/mL) GL MPs are reported as follows.

DSC-thermograms of GL MPs before and after NAC loading are illustrated in Figure 4a. Both DSC curves show an endothermic event in the temperature range of 60-120°C related to water evaporation from the MPs samples. Moreover, an exothermic event was registered at about 253°C for GL MPs and at about 240°C for NAC-loaded GL MPs due to the degradation of the natural polysaccharide. The obtained results suggest that the presence of the mucolytic agent promotes the thermal degradation of the microspheres by anticipating the degradation event.

Figure 4b shows TGA curves of unloaded GL MPs and NAC-loaded GL MPs, the differences in the trends would indicate the drug effect on GL MPs thermo-degradative behavior. In particular, the derivative curve of NAC-loaded GL MPs indicates two degradative events at about 250°C and 300°C, respectively. It can be reasonably assumed that the first peak was related to a thermal modification of GL due to the presence of NAC, whereas the second one to the degradation of NAC contained inside particles.

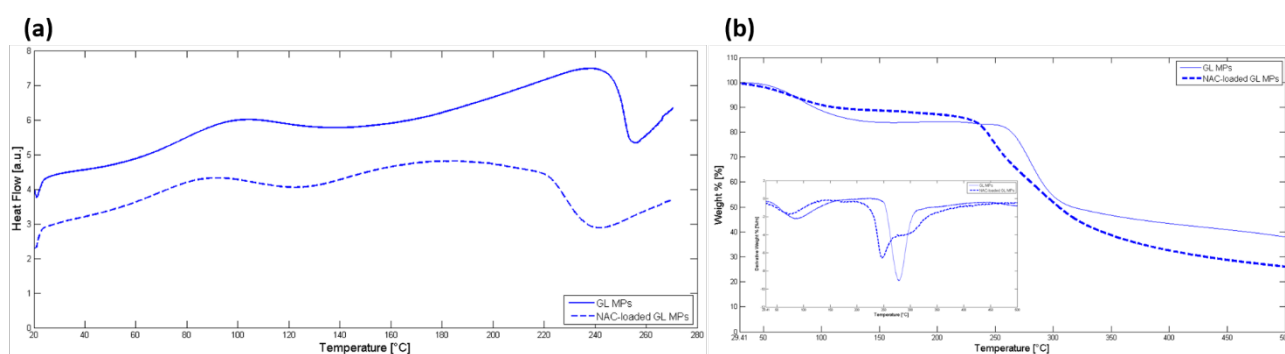


Fig.4 Characterizations of GL MPs unloaded and loaded with NAC: DSC-thermograms (a) and TGA curves (b). a.u.: arbitrary units; inset: second derivative traces obtained from TGA.

FT-IR investigation was performed on NAC-loaded GL MPs to evaluate the effective drug absorption on particles. IR spectra of GL MPs firstly showed the following typical absorption peaks: O-H stretching at 3.382 cm^{-1} , C-H stretching at 2.926 cm^{-1} , COO^- asymmetric stretching at 1.608 cm^{-1} , polysaccharide ring at 1.064 cm^{-1} . Afterwards, FT-IR chemical imaging investigation was carried out on GL microspheres incorporating the mucolytic drug. Figure 5 shows chemical maps and the corresponding media spectra for NAC-loaded GL MPs obtained both in μATR (Fig. 5a and b) and transmission (Fig. 5c and d) mode. The gained spectra confirmed the characteristic band of NAC at 1.727 cm^{-1} , thus demonstrating that the drug was loaded inside GL MPs.

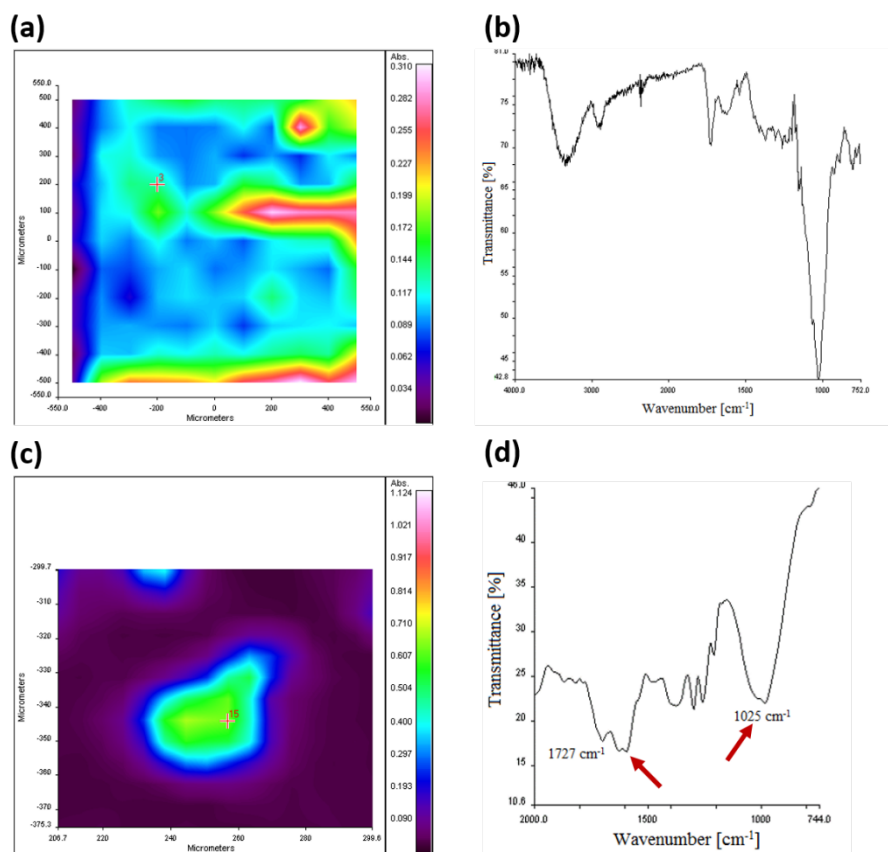


Fig.5 Chemical maps (a, c) and media spectra (b, d) of NAC-loaded GL MPs acquired in μ ATR mode (a, b) and transmission mode (c, d).

3.2 Release kinetics

The release kinetics of NAC by microspheres was evaluated by analyzing supernatants collected at prefixed times through HPLC. Figure 6 shows the amount of NAC released *per* micrograms of MPs as a function of time and for each concentration used in the absorption tests.

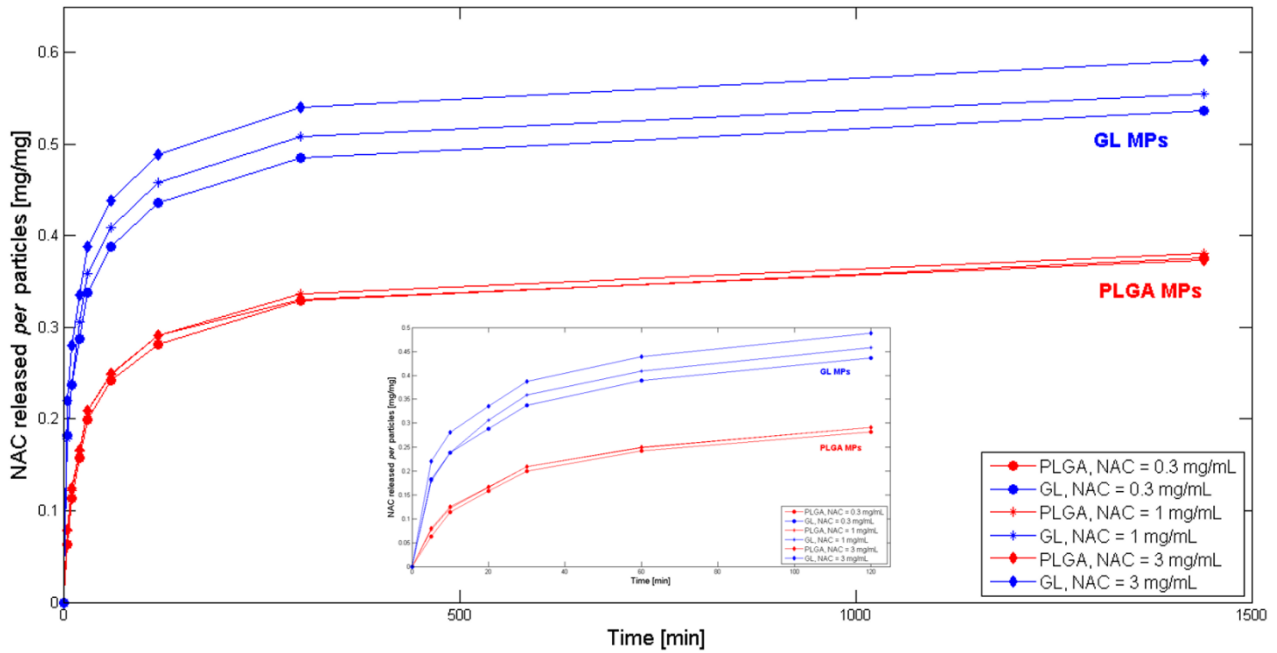


Fig.6 Release kinetics of NAC at three different concentrations from PLGA MPs and GL MPs.

The kinetics of drug release were rapid for both NAC-loaded PLGA and GL MPs with an elevated slope in the first 10 min. However, the total amount of NAC released by GL MPs resulted higher than that released from PLGA MPs independently of the concentration of the loaded NAC (i.e. 0.3, 1, 3 mg/mL). As a matter of fact, PLGA MPs showed a lower quantity of released drug which occurred in a more gradual and controlled manner. The obtained results were in agreement with the high swelling degree of GL MPs due to their porous structure and high hydrophilicity. On the other hand, PLGA MPs showed a high stability although it is a biodegradable polymer with a high degradation rate compared to other polyester aliphatic polymers (such as polycaprolactone or polylactic acid). Finally, it is worth noting that for GL MPs the higher the concentration of the loaded drug is, the greater is the amount of released NAC. This outcome further confirmed those achieved from the absorption tests showing that the amount of absorbed NAC increased with the increment of the tested drug concentration. Therefore, the attained results allowed us to select 3 mg/mL (w/v) as the concentration of NAC to be used in the rheological analysis. In conclusion, the results obtained in the present study revealed rapid release kinetics of NAC from both microcarriers that allow a fast action for inducing an early mucus degradation after MPs inhalation with the resulting penetration of anti-inflammatory agents.

3.3 *In vitro* biocompatibility of MPs

One of the main objectives of this study was the development of microcarriers able to penetrate the viscous and highly complex CF sputum without causing toxicity at pulmonary level. Within this aim,

in vitro cytocompatibility tests were performed and the effects of two different concentrations (namely 10 and 100 $\mu\text{g}/\text{mL}$) of both PLGA and GL MPs on human lung cancer cells (i.e. A549 cell line) viability and proliferation were evaluated. Figure 7a shows that A549 cell viability assessed by PI staining and flow cytometry was unchanged after 24, 48 and 72 h of treatment. A549 cell proliferation was therefore assessed at the same three time points by cell counting. Figure 7b illustrates a slight but not statistically significant difference between control and treated cells regardless of the tested polymeric MPs (i.e. PLGA and GL) and concentrations (i.e. 10 and 100 $\mu\text{g}/\text{mL}$), thus indicating that the produced MPs do not even interfere with the replicative capacity of the A549 cell line.

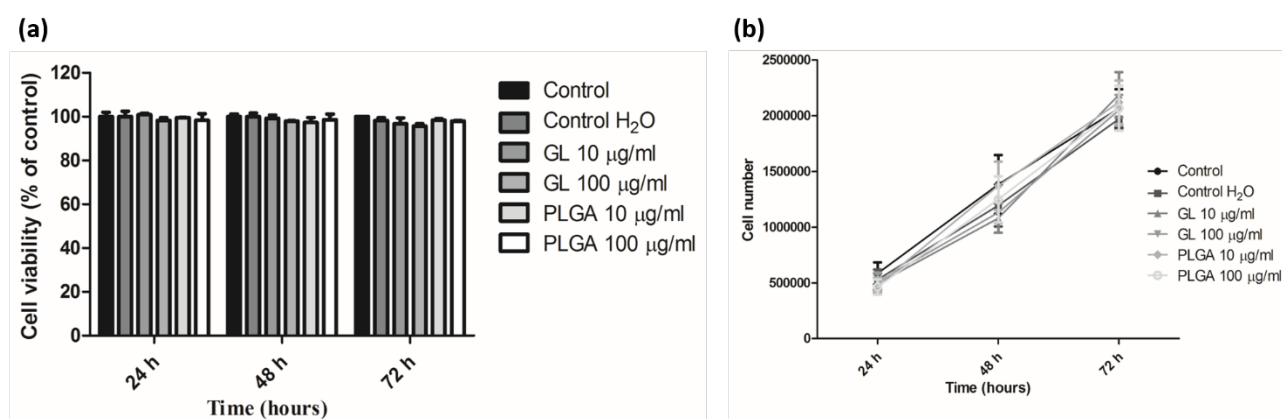


Fig.7 *In vitro* biocompatibility tests on A549 human lung cancer cells treated with PLGA MPs and GL MPs: cell viability (a) and proliferation (b). The results are expressed as mean (%) of control \pm SD, $n=3$.

In conclusion, neither the two MPs concentrations nor the two classes of tested polymers showed cytotoxic effects and thus both PLGA and GL MPs can be considered safe for human lung cells.

3.4 Mucolytic capability of MPs

To evaluate the effect of MPs on the degradation of CF mucus, AS was firstly produced and its rheological properties compared with sputum from CF patients by measuring the viscosity of sputum samples as a function of shear rate at 37°C (Figure 8).

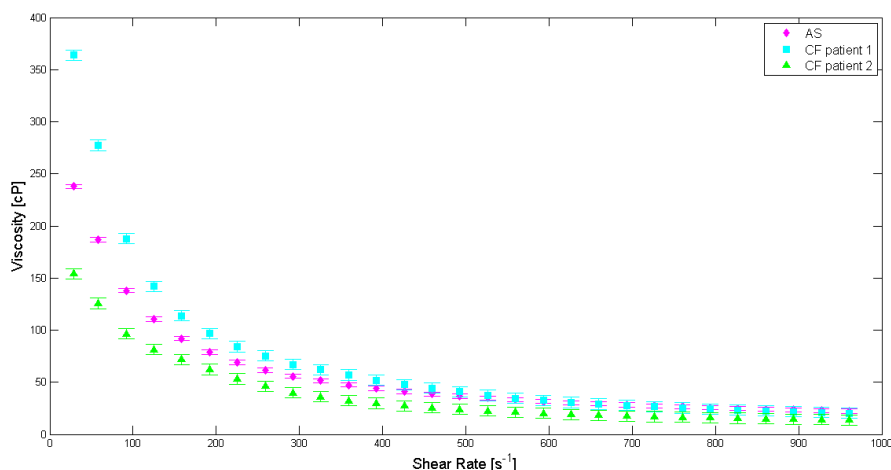


Fig.8 Comparison of mucus viscosity vs shear rate between AS and sputum from CF patients.

A reduction of the viscosity for both set of samples was found as the shear rate increased indicating a shear thinning behaviour. Moreover, the trends of viscosity for AS and CF sputum resulted comparable over the entire tested shear rate range. The gained findings therefore allowed to use AS for the successive rheological analysis.

Rheological analysis on various AS samples was finally carried out in order to assess the effect of the mucolytic agent on the AS viscosity after the addition of NAC-loaded (concentration of 3 mg/mL) MPs. In particular, the influence of the MPs-based drug delivery systems on AS degradation was evaluated by comparing viscosity vs shear rate of the following samples (Figure 9): pure AS, AS loaded with 5 mg/mL of PLGA or GL MPs without NAC, AS loaded with pure NAC and AS loaded with 5 mg/mL of PLGA or GL MPs containing NAC.

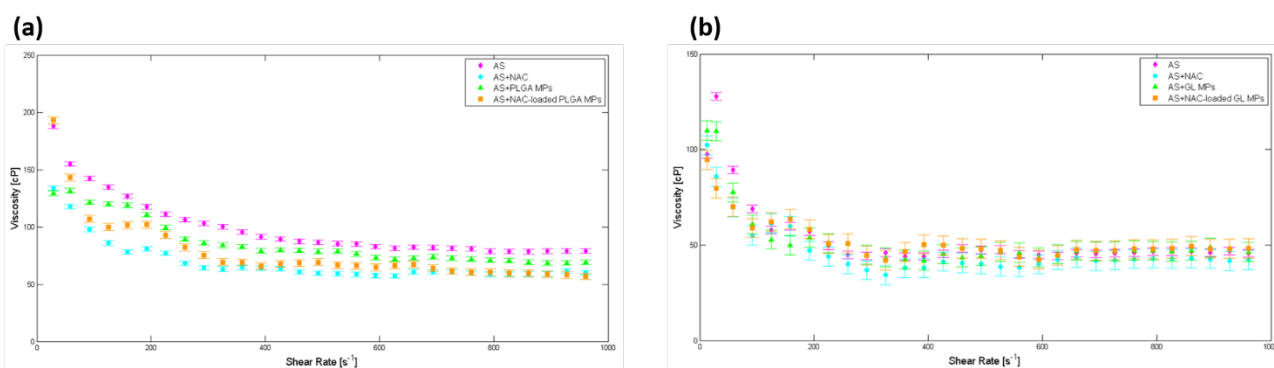


Fig.9 Viscosity measurements vs shear rate for samples based on PLGA MPs (a) and GL MPs (b).

Figure 9a shows viscosity measurements as a function of shear rates for samples based on PLGA MPs. A decrease of viscosity was detected for each of the tested samples when compared to pure AS. In particular, the highest viscosity reduction was achieved for AS after the addition of NAC, as

obviously expected from a mucolytic agent due to its specific biological activity. Interestingly, a lowering behavior of viscosity was also observed for AS following the addition of NAC-loaded PLGA MPs. The obtained result therefore suggests that the simultaneous action of the chemical structure of MPs and of the de-polymerizing agent could be exploited to better contrast the tenacious and high complex mucus of CF patients. Importantly, these results confirmed also the capability of MPs to release the loaded drug in a mucus-based medium. Finally, a reduction of viscosity was furthermore observed by adding pure PLGA MPs, hence confirming the use of this synthetic polymer as the right choice to develop microcarriers targeting CF mucus. The trend of viscosity *vs* shear rate for GL MPs are reported in Figure 9b. As found for PLGA-based samples, a similar behavior was also observed for GL carriers thus confirming the release and diffusion of NAC from MPs directly in the mucus.

4. Conclusions

Polymeric MPs were proposed as novel drug delivery systems with a mucolytic action for the pharmacological treatment of the CF lungs. In particular, PLGA MPs and GL MPs were synthesized by O/W and W/O techniques, respectively, which have been optimized to obtain suitable particles dimensions in agreement with the CF airway calibre and anatomy. PLGA and GL microspheres were therefore evaluated and successfully utilized as platforms for an efficient encapsulation, *in vitro* delivery and the following sustained release of NAC through the dense and tenacious CF mucus layer. *In vitro* biological tests also demonstrated that both kinds of MPs were cytocompatible. Interestingly, unloaded PLGA and GL MPs showed a reduction of viscosity compared to pure AS. However, the highest viscosity reduction was overall achieved for NAC-loaded microspheres, thus confirming the release of the depolymerising agent from particles and its diffusion directly into the mucus. In conclusion, the results obtained from the morphological, physico-chemical, biological and rheological characterizations of PLGA MPs and GL MPs loaded with the mucolytic agent suggest their potential as efficient vehicles for providing and improving local drug bioavailability (such as antibiotics and anti-inflammatory agents) in the treatment of CF.

Future works will concern the development of novel integrated and multifunctional drug delivery systems for targeting CF lung. In particular, the considered strategy will be based on the combination of MPs designed to efficiently reach and cross the mucus barrier, and smart nanosystems able to release specific drugs directly to the altered CF microenvironment for a better control of infection-inflammation processes. A successful combination of such micro- and nano-vectors would represent an innovative synergic and effective way to treat CF patients improving their compliance and quality of life.

Funding sources

This work was in part supported by Fondazione CRT [grant number 2016-079].

References

- [1] S. M. Rowe, S. Miller, E. J. Sorscher, Cystic fibrosis, *New Engl. J. Med.* 352 (2005) 1992–2001.
- [2] M. J. Hoegger, A. J. Fischer, J. D. McMenimen, L. S. Ostedgaard, A. J. Tucker, M. A. Awadalla, T. O. Moninger, A. S. Michalski, E. A. Hoffman, J. Zabner, et al., Impaired mucus detachment disrupts mucociliary transport in a piglet model of cystic fibrosis, *Science* 345 (2014) 818–822.
- [3] R. Boucher, New concepts of the pathogenesis of cystic fibrosis lung disease, *Eur. Respir. J.* 23 (2004) 146–158.
- [4] G. Döring, P. Flume, H. Heijerman, J. S. Elborn, C. S. Group, et al., Treatment of lung infection in patients with cystic fibrosis: current and future strategies, *J. Cyst. Fibros.* 11 (2012) 461–479.
- [5] D. S. Armstrong, K. Grimwood, R. Carzino, J. B. Carlin, A. Olinsky, P. D. Phelan, Lower respiratory infection and inflammation in infants with newly diagnosed cystic fibrosis, *BMJ-Brit. Med. J.* 310 (1995) 1571–1572.
- [6] D. S. Armstrong, S. M. Hook, K. M. Jansen, G. M. Nixon, R. Carzino, J. B. Carlin, C. F. Robertson, K. Grimwood, Lower airway inflammation in infants with cystic fibrosis detected by newborn screening, *Pediatr. Pulm.* 40 (2005) 500–510.
- [7] I. d’Angelo, C. Conte, M. I. La Rotonda, A. Miro, F. Quaglia, F. Ungaro, Improving the efficacy of inhaled drugs in cystic fibrosis: challenges and emerging drug delivery strategies, *Adv. Drug Deliver. Rev.* 75 (2014) 92–111.
- [8] B. M. Ibrahim, M. D. Tsifansky, Y. Yang, Y. Yeo, Challenges and advances in the development of inhalable drug formulations for cystic fibrosis lung disease, *Expert Opin. Drug Del.* 8 (2011) 451–466.
- [9] T. M. Murphy, B. J. Rosenstein, *Advances in the Science and Treatment of Cystic Fibrosis Lung Disease: A Continuing Medical Education Resource*, Duke University Medical Center & Health System, Durham, 1998.

- [10] K. Kunzelmann, M. Mall, Pharmacotherapy of the ion transport defect in cystic fibrosis, *Clin. Exp. Pharmacol.* P. 28 (2001) 857–867.
- [11] B. K. Rubin, Emerging therapies for cystic fibrosis lung disease, *CHEST* 115 (1999) 1120–1126.
- [12] N. Høiby, H. K. Johansen, C. Moser, Z. Song, O. Ciofu, A. Kharazmi, *Pseudomonas aeruginosa* and the in vitro and in vivo biofilm mode of growth, *Microbes Infect.* 3 (2001) 23–35.
- [13] M. C. Walters, F. Roe, A. Bugnicourt, M. J. Franklin, P. S. Stewart, Contributions of antibiotic penetration, oxygen limitation, and low metabolic activity to tolerance of *Pseudomonas aeruginosa* biofilms to ciprofloxacin and tobramycin, *Antimicrob. Agents Ch.* 47 (2003) 317–323.
- [14] W.-C. Chiang, M. Nilsson, P. Ø. Jensen, N. Høiby, T. E. Nielsen, M. Givskov, T. Tolker-Nielsen, Extracellular DNA shields against aminoglycosides in *Pseudomonas aeruginosa* biofilms, *Antimicrob. Agents Ch.* 57 (2013) 2352–2361.
- [15] S. M. Moskowitz, J. M. Foster, J. Emerson, J. L. Burns, Clinically feasible biofilm susceptibility assay for isolates of *Pseudomonas aeruginosa* from patients with cystic fibrosis, *J. Clin. Microbiol.* 42 (2004) 1915–1922.
- [16] T. Moriarty, J. McElnay, J. Elborn, M. Tunney, Sputum antibiotic concentrations: implications for treatment of cystic fibrosis lung infection, *Pediatr. Pulm.* 42 (2007) 1008–1017.
- [17] W. Hengzhuang, H. Wu, O. Ciofu, Z. Song, N. Høiby, Pharmacokinetics/pharmacodynamics of colistin and imipenem on mucoid and nonmucoid *Pseudomonas aeruginosa* biofilms, *Antimicrob. Agents Ch.* 55 (2011) 4469–4474.
- [18] W. Hengzhuang, H. Wu, O. Ciofu, Z. Song, N. Høiby, In vivo pharmacokinetics/pharmacodynamics of colistin and imipenem in *Pseudomonas aeruginosa* biofilm infection, *Antimicrob. Agents Ch.* 56 (2012) 2683–2690.
- [19] W. Hengzhuang, O. Ciofu, L. Yang, H. Wu, Z. Song, A. Oliver, N. Høiby, High β -lactamase levels change the pharmacodynamics of β -lactam antibiotics in *Pseudomonas aeruginosa* biofilms, *Antimicrob. Agents Ch.* 57 (2013) 196–204.
- [20] J. R. Riordan, J. M. Rommens, B.-s. Kerem, N. Alon, R. Rozmahel, Z. Grzelczak, J. Zielenski, S. Lok, N. Plavsic, J.-L. Chou, et al., Identification of the cystic fibrosis gene: cloning and characterization of complementary DNA, *Science* 245 (1989) 1066–1073.

- [21] N. Derichs, Targeting a genetic defect: cystic fibrosis transmembrane conductance regulator modulators in cystic fibrosis, *Eur. Respir. Rev.* 22 (2013) 58–65.
- [22] J. Hanes, J. Demeester, Drug and gene delivery to mucosal tissues: the mucus barrier, *Adv. Drug Deliver. Rev.* 2 (2009) 73–74.
- [23] B. Dhooghe, S. Noël, F. Huaux, T. Leal, Lung inflammation in cystic fibrosis: pathogenesis and novel therapies, *Clin. Biochem.* 47 (2014) 539–546.
- [24] N. Sanders, C. Rudolph, K. Braeckmans, S. C. De Smedt, J. Demeester, Extracellular barriers in respiratory gene therapy, *Adv. Drug Deliver. Rev.* 61 (2009) 115–127.
- [25] C. T. Vogelson, Advances in drug delivery systems, *Mod. Drug Discov.* 4 (2001) 49–50.
- [26] P. D. Reddy, D. Swarnalatha, Recent advances in novel drug delivery systems, *Int. J. PharmTech Res.* 2 (2010) 2025–2027.
- [27] T. K. Dash, V. B. Konkimalla, Poly-epsilon-caprolactone based formulations for drug delivery and tissue engineering: A review, *J. Control. Release* 158 (2012) 15–33.
- [28] V. K. Rai, N. Mishra, A. K. Agrawal, S. Jain, N. P. Yadav, Novel drug delivery system: an immense hope for diabetics, *Drug Deliv.* 23 (2016) 2371–2390.
- [29] J. Hsu, S. Muro, Nanomedicine and drug delivery strategies for treatment of genetic diseases, in *Human genetic diseases*, InTech, Rijeka, 2011.
- [30] H. Grasmann, F. Ratjen, Emerging therapies for cystic fibrosis lung disease, *Expert Opin. Emerg. Dr.* 15 (2010) 653–659.
- [31] B. D. Kurmi, J. Kayat, V. Gajbhiye, R. K. Tekade, N. K. Jain, Micro-and nanocarrier-mediated lung targeting, *Expert Opin. Drug Del.* 7 (2010) 781–794.
- [32] Z. Mohammadi, F. Dorkoosh, S. Hosseinkhani, K. Gilani, T. Amini, A. R. Najafabadi, M. R. Tehrani, In vivo transfection study of chitosan-dna-fap-b nanoparticles as a new non viral vector for gene delivery to the lung, *Int. J. Pharm.* 421 (2011) 183–188.
- [33] N. J. Boylan, A. J. Kim, J. S. Suk, P. Adstamongkonkul, B. W. Simons, S. K. Lai, M. J. Cooper, J. Hanes, Enhancement of airway gene transfer by dna nanoparticles using a ph-responsive block copolymer of polyethylene glycol and poly-l-lysine, *Biomaterials* 33 (2012) 2361–2371.
- [34] D. Cipolla, I. Gonda, H.-K. Chan, Liposomal formulations for inhalation, *Ther. Deliv.* 4 (2013) 1047–1072.

- [35] M. Gaspar, W. Couet, J.-C. Olivier, A. Pais, J. Sousa, Pseudomonas aeruginosa infection in cystic fibrosis lung disease and new perspectives of treatment: a review, *Eur. J. Clin. Microbiol.* 32 (2013) 1231–1252.
- [36] R. Savla, T. Minko, Nanotechnology approaches for inhalation treatment of fibrosis, *J. Drug Target.* 21 (2013) 914–925.
- [37] V. Sinha, A. Singla, S. Wadhawan, R. Kaushik, R. Kumria, K. Bansal, S. Dhawan, Chitosan microspheres as a potential carrier for drugs, *Int. J. Pharm.* 274 (2004) 1–33.
- [38] M. Rekha, C. P. Sharma, Synthesis and evaluation of lauryl succinyl chitosan particles towards oral insulin delivery and absorption, *J. Control. Release* 135 (2009) 144–151.
- [39] A. D. Sezer, E. Cevher, Topical drug delivery using chitosan nano- and microparticles, *Expert Opin. Drug Del.* 9 (2012) 1129–1146.
- [40] M. S. Mesiha, M. B. Sidhom, B. Fasipe, Oral and subcutaneous absorption of insulin poly (isobutylcyanoacrylate) nanoparticles, *Int. J. Pharm.* 288 (2005) 289–293.
- [41] X. Zhang, H. Zhang, Z. Wu, Z. Wang, H. Niu, C. Li, Nasal absorption enhancement of insulin using peg-grafted chitosan nanoparticles, *Eur. J. Pharm. Biopharm.* 68 (2008) 526–534.
- [42] M. O. Henke, F. Ratjen, Mucolytics in cystic fibrosis, *Paediatr. Respir. Rev.* 8 (2007) 24–29.
- [43] P. Agent, H. Parrott, Inhaled therapy in cystic fibrosis: agents, devices and regimens, *Breathe* 11 (2015) 110–118.
- [44] Y. Yang, M. D. Tsifansky, S. Shin, Q. Lin, Y. Yeo, Mannitol-guided delivery of ciprofloxacin in artificial cystic fibrosis mucus model, *Biotechnol. Bioeng.* 108 (2011) 1441–1449.
- [45] A. Sheffner, E. Medler, L. Jacobs, H. Sarett, The in vitro reduction in viscosity of human tracheobronchial secretions by acetylcysteine, *Am. Rev. Respir. Dis.* 90 (1964) 721–729.
- [46] J. S. Suk, S. K. Lai, N. J. Boylan, M. R. Dawson, M. P. Boyle, J. Hanes, Rapid transport of muco-inert nanoparticles in cystic fibrosis sputum treated with n-acetyl cysteine, *Nanomedicine-UK* 6 (2011) 365–375.
- [47] M. Kesimer, C. Ehre, K. A. Burns, C. W. Davis, J. K. Sheehan, R. J. Pickles, Molecular organization of the mucins and glycocalyx underlying mucus transport over mucosal surfaces of the airways, *Mucosal Immunol.* 6 (2013) 379.

- [48] S. Sartori, A. Caporale, A. Rechichi, D. Cufari, C. Cristallini, N. Barbani, P. Giusti, G. Ciardelli, Biodegradable paclitaxel-loaded microparticles prepared from novel block copolymers: influence of polymer composition on drug encapsulation and release, *J. Pept. Sci.* 19 (2013) 205–213.
- [49] N. Barbani, C. Cristallini, R. Pulizzi, M. Donati, M. Gagliardi, A. Rechichi, G. D. Guerra, P. Giusti, Preparation and functional characterization of a polysaccharidic matrix microsphere-shaped for controlled drug release, *J. Appl. Biomater. Biom.* (2009) 54.
- [50] B. M. Ibrahim, S. Park, B. Han, Y. Yeo, A strategy to deliver genes to cystic fibrosis lungs: a battle with environment, *J. Control. Release* 155 (2011) 289–295.
- [51] N. Labiris, M. Dolovich, Pulmonary drug delivery. Part I: physiological factors affecting therapeutic effectiveness of aerosolized medications, *Brit. J. Clin. Pharmacol.* 56 (2003) 588–599.
- [52] L. Gradon, J. Marijnissen, Optimization of aerosol drug delivery, Springer Science & Business Media, 2003.
- [53] D. E. Geller, J. Weers, S. Heurding, Development of an inhaled dry-powder formulation of tobramycin using pulmosphere™ technology, *J. Aerosol Med. Pulm. D.* 24 (2011) 175–182.
- [54] C. Loira-Pastoriza, J. Todoroff, R. Vanbever, Delivery strategies for sustained drug release in the lungs, *Adv. Drug Deliver. Rev.* 75 (2014) 81–91.